

THE EFFECT OF POWER SUPPLY RIPPLE ON DC WATER ELECTROLYSIS EFFICIENCY

ZSOLT DOBÓ¹–ÁRPÁD BENCE PALOTÁS²–PÁL TÓTH³

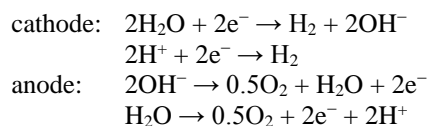
It has been known that the efficiency of alkaline water electrolysis under DC conditions is dependent on the stability of the power supply. High output voltage fluctuation is typical mostly at thyristor-based power supplies - this effect is known as power supply ripple. As a result of continuously varying voltage levels the behaviour of the electrolysis may differ from DC conditions. The deviation from DC signals may lead to decreased cell efficiency – the magnitude of this effect was investigated in this paper. A novel experimental method was designed in order to obtain a complete experimental matrix. The experimental method was based on a fully automatic, programmable power supply and measurement system. The system was capable of carrying out thousands of measurements in a day without human supervision. Cell efficiency was recorded as a function of signal amplitude and frequency, while signal offset (the DC component) was kept at a constant 2.44 V. A total of 245 measurements were carried out that investigated an experimental matrix between 0.2 and 5 kHz frequency and between 0 and 443 mV amplitude. It was shown that cell efficiency was not significantly affected by signal frequency, while a significant efficiency loss (up to 4%) was measured as the amplitude of signal variation increased.

Keywords: water electrolysis, voltage fluctuation, cell efficiency

Introduction

Hydrogen is mostly produced from fossil resources, primarily from methane (natural gas) [1] due to cost-efficiency reasons. However, growing concerns about diminishing fossil fuel reserves and increasing gas prices drive attention to hydrogen production from water. The conventional electrolytic method for hydrogen production is alkaline water electrolysis. Net efficiency of 50 to 60% is common with current electrolytic hydrogen production methods [1, 2, 3], however the overall efficiency is much lower if the losses of electricity generation from primer or renewable fuels is also taken into consideration. In this case the overall efficiency rate would hardly reach 40% [4]. Because of the low overall efficiency, attention turned to enhancing the electrolytic process; i.e. by subjecting the cell to a gravity field [5], ultrasonic waves [6] or magnetic fields [7].

The conventional DC electrolysis of water involves generation of hydrogen gas at the cathode and oxygen gas at the anode. The electrode reactions are typically described as follows [8]:



¹ University of Miskolc, Department of Combustion Technology and Thermal Energy
3515 Miskolc-Egyetemváros, Hungary
zsoltdobo@gmail.com

² University of Miskolc, Department of Combustion Technology and Thermal Energy
3515 Miskolc-Egyetemváros, Hungary
arpad.palotas@uni-miskolc.hu

³ University of Miskolc, Department of Combustion Technology and Thermal Energy
3515 Miskolc-Egyetemváros, Hungary
toth.pal@uni-miskolc.hu

Gas formation can be induced by applying a potential difference between the cell electrodes. In theory, the thermodynamic decomposition voltage of water at 298 K and 1 atm is 1.23 V, however, due to reaction overpotentials and resistance losses (ohmic voltage drop), higher cell voltages should be applied [8]. Gas starts to form at a voltage level of 1.65–1.7 V and most industrial cells are operated from 1.8 to 2.6 V [4, 9].

In order to create a potential difference between the electrodes AC/DC or DC/DC power supplies are typically used. One of the main properties of power supplies is voltage ripple, meaning that the voltage level is not constant, but oscillates around a mean value. Reduced or eliminated voltage ripple is an important requirement, although it is difficult to achieve with high-power sources. In water electrolysis any deviation from perfectly uniform DC voltage might affect the electric power consumption, the intensity of gas production and the water splitting efficiency. Although several papers reported using impulse voltage or interrupted direct current [10–13], the available information about the effects of the applied voltage waveforms is still scarce [14, 15]. It has been suggested that efficiency loss may occur if the power supply used for DC electrolysis produces contaminated or unstable signals [16], but the magnitude of this effect has not been investigated so far. Since the feasibility of alkaline DC water electrolysis depends strongly on the achievable cell efficiency, the information regarding the effect of signal stability on efficiency may be valuable from economic points of view. In this paper, we investigate the effect of power supply ripple on cell efficiency. A novel experimental system was designed and built that allowed for the quick and automatic assessment of different signal waveforms that modelled the ripple of DC power supplies.

1. Materials and methods

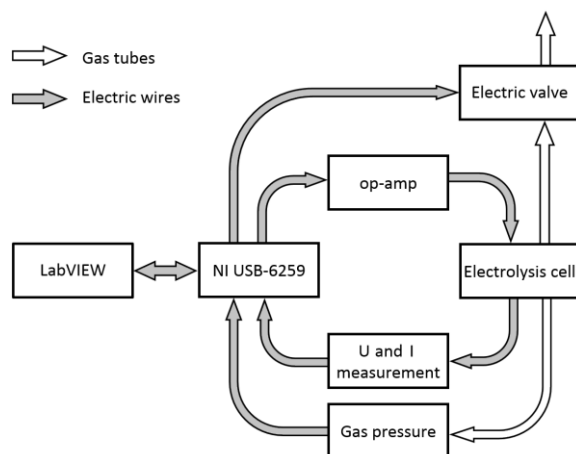


Figure 1
Schematic illustration of the experimental system

A schematic illustration of the measurement system is seen in Figure 1. The main component is the gas-tight cell powered by a special power supply containing a high current operational amplifier (op-amp) type OPA549 [17]. The op-amp is controlled by a dedicated National Instruments device (NI USB-6259) – its operation can be automated using a LabVIEW program. The device is responsible for measuring cell voltage, cell current and the pressure of the generated gas. The NI device can also control the electric valve connected to the top

of cell. This system can generate arbitrary waveforms with frequencies up to 50 kHz, currents up to 8 A and between voltages of -10 and 10 V. The power supply can be operated either in galvanostatic or potentiostatic mode, i.e., it is able to generate voltage or current waveforms, according to the operational amplifier topology [17].

The power supply is connected to the electrolytic cell shown in Figure 2. The cell is a gas-tight vessel with two electrodes attached to the lid. Next to the electrodes are the two gas outlets, a T-type Thermocouple (used as a sensor to measure electrolyte temperature) and the outlet pipes of the cooling cycle (mounted on the lid). Two 1.5 mm thick stainless steel electrodes (material: EN 1.4307) were placed in the cell, with a spacing of 40 mm. 500 ml of 30 wt% potassium hydroxide aqueous solution was used as the electrolyte. The temperature of the electrolyte was 25 ± 0.5 °C.

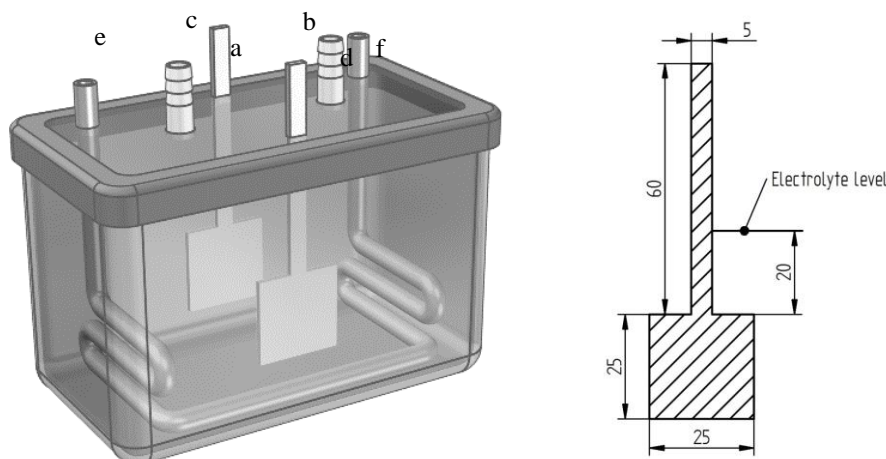


Figure 2

Left: Schematic illustration of the electrolytic cell, a) cathode, b) anode, c) to pressure sensor, d) to valve, e) cooling water inlet, f) cooling water outlet

Right: electrode dimensions and their position in the electrolyte (the units are in mm)

The gas bubbles formed at the electrode surfaces cause pressure increase in the cell. The rate of pressure increase is directly proportional to the flow rate of the gas produced. Pressure was measured using a pressure sensor type MPX5010DP (Freescale Semiconductor, Inc.), capable of measuring differential pressures up to 10 kPa at a sensitivity of 450 mV/kPa. The pressure sensor was calibrated by using an independent flow meter. While the pressure sensor was fixed at one of the gas outlets, the second gas outlet was connected to an electromagnetic valve. When the valve is open the pressure in the cell decreases to the ambient pressure and the H_2+O_2 gas mixture is released into the environment. The pressure increase in a single experiment is negligible; however, over a long series of experiments, pressure can build up in the cell, which may alter electrolysis conditions. The formed gas is therefore released through the valve after each experiment. The valve can be operated via the digital output terminal of the signal generator module.

The fully automated measurement system allows for carrying out a large number of water splitting experiments within a short timeframe, which facilitates the systematic exploration of frequency and amplitude effects on cell efficiency. The system is also remote-controlled, allowing for changes in experimental conditions and sampling through the internet.

Power supply ripple was modelled by applying sinusoidal waveforms between the electrodes with constant offset (DC component) and varying frequency and amplitude. Frequency was changed from 200 Hz to 5000 Hz in 100 Hz increments, while amplitude was varied from 0 mV to 440 mV in 110 mV increments. The experimental matrix therefore contained 245 cases, of which 49 were true DC cases. The offset value of the waveforms was $2436 \text{ mV} \pm 12 \text{ mV}$.

The duration of each measurement was 15 s. After completing a case, the magnetic valve was opened for 15 s and the cell was allowed to equilibrate for an additional 30 s.

Cell voltage, cell current and cell pressure were measured and recorded at a sampling rate of 50 kHz – this sampling frequency allowed for the bias-free measurement of waveform parameters. Data analysis was performed by custom software developed in C#. The custom software calculated gas flow rate and power consumption from the measured raw data. Flow rate was calculated based on the rate of linear pressure rise during an experiment, while power consumption was computed as:

$$P = \int U(t)I(t)dt \quad (1)$$

where P is power, U is the measured cell voltage and I is the measured cell current. The efficiency of water splitting (η) was calculated as the ratio of measured and theoretical gas flow rate using Faraday's law:

$$\eta = 100Q \left[\frac{V_m P}{U^0 F} \left(\frac{1}{z_{H_2}} + \frac{1}{z_{O_2}} \right) \right]^{-1} \quad (2)$$

where Q is the measured gas flow rate (derived from pressure rise), V_m is the molar volume of ideal gases at standard conditions ($24465 \text{ cm}^3/\text{mol}$), U^0 is the theoretical thermodynamic decomposition voltage of water (1.23 V), F is Faraday's number (96485 C/mol) and z is charge number (2 for H_2 and 4 for O_2). All flow rates were evaluated at standard state (25°C , atmospheric pressure).

2. Results and discussion

Figure 3 shows the results of the 245 systematic experiments that were carried out by using the automatic system described in Section 1. It is seen that increasing the amplitude of voltage variation immediately resulted in decreasing efficiency. An increase in ripple magnitude from 0 to 443 mV resulted in an efficiency drop of about 4%. When expressed as relative magnitude, an amplitude of 443 mV corresponds to a root mean square (rms) variation of 13%, which may not be unreasonably high in an industrial setting (see Section 3.1 for details).

From Figure 3 it is also seen that the obtained efficiency values were not significantly affected by the frequency of the model waveforms, at least in the studied 0.2–5 kHz range. Figure 4 therefore shows cell efficiency along with other cell parameters as values averaged over the frequency range, in order to better show the effect of increasing signal amplitude. As seen, efficiency dropped about 4% as amplitude was increased. Cell current and gas flow rate increased very slightly with increasing amplitude – an increase of about 3% was

measured. Electric power intake, on the other hand, increased from 4.4 to 4.9 W as amplitude was increased from 0 to 443 mV, which is a relative change of about 11%. This shows, that the decrease of efficiency was mainly caused by the significantly increased power intake.

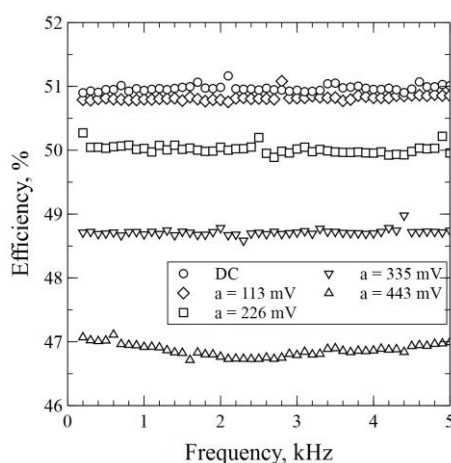


Figure 3

Efficiency as a function of the frequency and amplitude of the AC component of the model waveform. A total of 5 different amplitude setting were tested, of which the first corresponded to the true DC case ($a = 0$). Efficiency was reduced from about 51% to 47% as the magnitude of voltage ripple increased from 0 to 443 mV

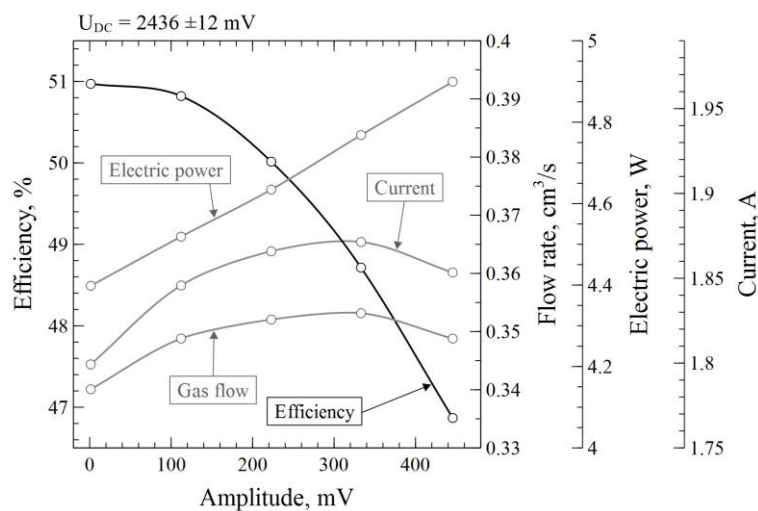


Figure 4

Water splitting efficiency, cell current, gas flow rate and electric power consumption as function of signal amplitude. The figure shows that efficiency dropped about 4% as signal amplitude increased from 0 to 443 mV. The frequency dependence of the obtained values was negligible – the standard errors of the mean values were so low that error bars are not shown in the figure. The data shown here demonstrates that the efficiency drop was mostly caused by the increased power intake of the cell. Gas flow rate remained proportional to cell current

The data show that in the investigated frequency and amplitude range, the mass transfer and electrochemistry of the process did not change considerably. Efficiency was rather decreased by the increased power intake of the cell, which was caused by the oscillation of voltage and current. If the voltage and current signals are expressed as the superposition of a DC and AC component (assuming that there is a phase shift Φ relative to the voltage signal):

$$\begin{aligned} U &= U_{DC} + u = U_{DC} + a_U \sin(\omega t) \\ I &= I_{DC} + i = I_{DC} + a_I \sin(\omega t + \phi) \end{aligned} \quad (3)$$

where the index DC means the constant component, ω is radial frequency, t is time and a_U and a_I are the amplitudes, the power increase ΔP over the direct current case is the integral of the two time-varying components:

$$\Delta P = \frac{a_I a_U}{2} \quad (4)$$

When carrying out the correction of measured power by Equation 4, the drop in energy efficiency indeed proved to be around 4%, justifying our previous statement about the main cause of the efficiency drop.

By looking at the current efficiency, expressed as:

$$\eta_I = 100Q \left[\frac{V_m I}{F} \left(\frac{1}{z_{H_2}} + \frac{1}{z_{O_2}} \right) \right]^{-1} \quad (5)$$

it was observed that η_I decreased from approximately 99.7% to 99.1% as amplitude increased. The very slight change indicates that the electrochemistry of the system was not changed much by increased ripple magnitude in the studied limits.

By looking at the measured voltage and current signals, a phase shift was observed, which is shown in Figure 5.

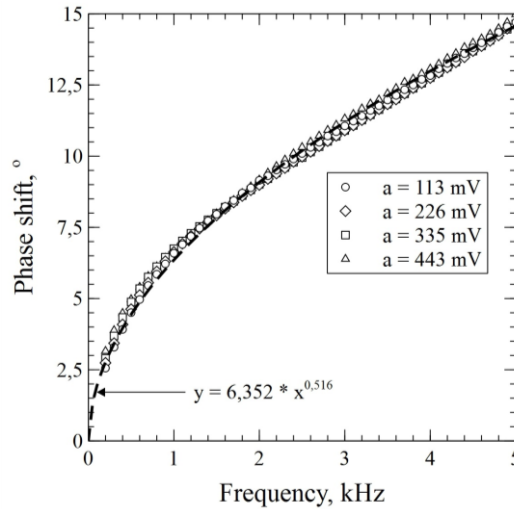


Figure 5

Phase shift between cell voltage and current. The phase shift increased with increasing frequency, but was fairly independent of ripple amplitude

As seen, the phase shift between voltage and current signals increased with increasing frequency, but was unchanged by increasing ripple amplitude. This indicates the capacitive behavior of the cell, while also pointing out that the effect of phase shift on cell power was not noticeable in the frequency limits investigated in this work. At higher frequencies, phase shift might affect cell efficiency. Further studies using the experimental system described in this paper may elaborate.

3. Notes on power supplies

Common silicon controlled rectifier (SCR) regulation techniques permit the design of low cost, compact power supplies, but their main disadvantage is relatively high ripple and noise [18]. For example a single phase, unfiltered, full-wave DC rectifier used in low power applications has around 48% rms ripple [19] at frequency 100 Hz, and a 3-phase rectifier used in high power applications has around 5% rms [20] at frequency 300 Hz. With inverter-grade thyristors the frequency can be increased to 600 Hz [21]. By reducing the output power in unfiltered 3-phase thyristor controlled rectifiers, the output ripple significantly grows – at 50% output power the ripple is around 40% rms [22]. Publications show that the voltage ripple can reach up to 60% rms [23]. To put these numbers into perspective, the highest magnitude ripple studied in this work was around 13%, which resulted in an energy efficiency loss of 4%. Although the ripple of the power supplies are mostly given for output voltage, in order to calculate or appreciate the efficiency loss the ripple of the electric current must also be known, what depends basically on the load.

By adding filters to a thyristor based rectifier the ripple can be reduced to 0.8% rms at full load, and a ripple of 2.8% rms is typical at 50% power [22]. According to our results, a ripple of similar magnitude causes an efficiency drop of 0.15%. By adding a filter to an SCR the ripple is lower, however, the overall cost of the power supply increase. The transistor based power supplies operates at much higher frequencies (from 5–10 kHz) than SCR, and their ripple is significantly lower, but the disadvantages are the higher cost and their usage in high power applications are not fully formed as yet.

Considering the strict requirements regarding energy efficiency in order to make water electrolysis a feasible technique for sustainable hydrogen production, it is therefore advisable to design electrolysis systems with an emphasized consideration of power supply stability. Since the rms ripple of typical power supplies increase when the unit is operated sub peak power, it is also advisable to avoid such modes of operation or provide other means to maintain cell efficiency at reduced powers.

Summary

The effect of power supply ripple on the efficiency of alkaline water electrolysis for hydrogen production was investigated. For the study, a novel, automated measurement system was used, that allowed for the remote collection of data from thousands of programmed experiments. Power supply ripple was modelled by applying sinusoidal voltage to an electrolysis cell. The voltage signals had a constant offset (DC component) and an alternating component with variable frequency and amplitude. A frequency range of 200–5000 Hz and an amplitude range of 0–443 mV was studied at an offset of 2.44 V. Results showed that the energy efficiency of the electrolysis process was not affected significantly by the source frequency, but was affected by the amplitude (the magnitude of the ripple). Cell efficiency dropped from 51% to 47% when the signal amplitude was increased from 0 to 443 mV (0–13% rms). The efficiency loss was mostly caused by the increased power consumption of the

cell, due to the effective power of the alternating components of voltage and current signals. Observations regarding current efficiency supported this conclusion, as current efficiency did not change much with increasing signal amplitude. The phase shift between cell voltage and current did not have a noticeable effect on cell efficiency in the studied frequency range. The results suggest that power supply signal stability must be an important factor in designing alkaline water electrolysis units, as typical ripple magnitudes may lead to significant efficiency drop.

Acknowledgement

This research was (partially) carried out in the framework of the Center of Excellence of Sustainable Resource Management at the University of Miskolc.

References

- [1] HOLLADAY, J. D.–HU, J.–KING, D. L.–WANG, Y.: An overview of hydrogen production technologies. *Catalysis Today*, 139, 2009, 244–260.
- [2] TURNER, J.–SVERDRUP, G.–MANN, M. K.–MANESS, P. C.–KROPOSKI, B.–GHIRARDI, M.–EVANS, R. J.–BLAKE, D.: Renewable hydrogen production. *International Journal of Energy Research*, 32, 2008, 379–407.
- [3] GRIMES, C. A.–VARGHESE, O. K.–RANJAN, S.: *Light, Water, Hydrogen – The solar generation of hydrogen by water photoelectrolysis*. Springer, 2008.
- [4] NIKOLIC, V. M.–TASIC, G. S.–MAKSIC, A. D.–SAPONJIC, D. P.–MILOVIC, S. M.–KANINSKI, M. P. M.: Raising efficiency of hydrogen generation from alkaline water electrolysis – Energy saving. *International Journal of Hydrogen Energy*, 35, 2010, 12369–12373.
- [5] WANG, M.–WANG, Z.–GUO, Z.: Water electrolysis enhanced by super gravity field for hydrogen production. *International Journal of Hydrogen Energy*, 35, 2010, 3198–3205.
- [6] LI, S.–D.–WANG, C.–C.–CHEN, C.–Y.: Water electrolysis in the presence of an ultrasonic field. *Electrochimica Acta*, 54, 2009, 3877–3883.
- [7] LIN, M.–Y.–HOURNG, L.–W.–KUO C.–W.: The effect of magnetic force on hydrogen production efficiency in water electrolysis. *International Journal of Hydrogen Energy*, 37, 2012, 1311–1320.
- [8] MARINI, S.–SALVI, P.–NELLI, P.–PESENTI, R.–VILLA, M.–BERRETTONI, M.–ZANGARI, G.–KIROS, Y.: Advanced alkaline water electrolysis. *Electrochimica Acta*, 82, 2012, 384–391.
- [9] WANG, M.–WANG, Z.–GONG, X.–GUO, Z.: The intensification technologies to water electrolysis – A review. *Renewable and Sustainable Energy Reviews*, 29, 2014, 573–588.
- [10] MAZLOOMI, K.–SULAIMAN, N.–AHMAD, S. A.–YUNUS, N. A.: Analysis of the frequency response of a water electrolysis cell. *International Journal of Electrochemical Science*, 8, 2013, 3731–3739.
- [11] SHIMIZU, N.–HOTTA, S.–SEKIYA, T.–ODA, O.: A novel method of hydrogen generation by water electrolysis using an ultra-short-pulse power supply. *Journal of Applied Electrochemistry*, 36, 2006, 419–423.
- [12] VANAGS, M.–KLEPERIS, J.–BAJARS, G.: *Water electrolysis with inductive voltage pulses. Electrolysis*. Chapter 2. Published by InTech, 2012.
- [13] SHAABAN, A. H.: *Pulsed DC and anode depolarization in water electrolysis for hydrogen generation*. HQ air force civil engineering support agency, final report, 1994.
- [14] MAZLOOMI, S. K.–SULAIMAN, N.: Influencing factors of water electrolysis electrical efficiency. *Renewable and Sustainable Energy Reviews*, 16, 2012, 4257–4263.
- [15] MAZLOOMI, K.–SULAIMAN, N. B.–MOAYEDI, H.: Electrical efficiency of electrolytic hydrogen production. *International Journal of Electrochemical Science*, 7, 2012, 3314–3326.
- [16] URSÚA, A.–MARROYO, L.–GUBÍA, E.–GANDÍA, L. M.–DIÉGUEZ, P. M.–SANCHIS, P.: Influence of the power supply on the energy efficiency of an alkaline water electrolyser. *International Journal of Hydrogen Energy*, 34, 2009, 3221–3233.

- [17] OPA549 type operational amplifier, technical datasheet (2016. 04. 06.)
<http://www.ti.com/lit/ds/symlink/opa549.pdf>
- [18] A. Technologies: *DC power supply handbook* (2016. 04. 06.)
<http://educyclopedia.karadimov.info/library/DC%20Power%20Supply%20Handbook.pdf>
- [19] MENTONE, P. F.: Pulse vs. DC plating: Knowing how and when to use each system is critical for producing plated metals. *Metal Finishing*, 103, 2005, 14–18.
- [20] SMITH, C. C.–CAMBRIA, P.: DC power supplies. *Metal Finishing*, 97, 1999, 679–702.
- [21] SINGH, M. D.–KHANCHANDANI, K. B.: *Power Electronics*. McGraw-Hill, 2008.
- [22] What is ripple? (2016. 04. 06.)
http://www.controlledpwr.com/whitepapers/ripple_formula.pdf
- [23] STEIN, B.: Effects of voltage ripple on plating uniformity in chloride zinc baths. *Metal Finishing*, 93, 1995, 100–103.